Consideration of magnetic field fluctuation measurements in torus plasma with a heavy ion beam probe

A. Shimizu[a] and A. Fujisawa
National Institute for Fusion Science, Oroshi-cho, Toki-shi, Gifu 509-5292, Japan

S. Ohshima
Nagoya University, Furo-cho, Chikusa-ku, Nagoya 464-0814, Japan

H. Nakano
Graduate University for Advanced Studies, Toki-shi, Gifu 509-5292, Japan

(Received 26 January 2004; accepted 21 December 2004; published online 1 April 2005)

The article proposes a method of magnetic fluctuation measurement using a heavy ion beam probe (HIBP) in an axisymmetric torus configuration. The method is based on the detection of the toroidal position (not velocity) of the secondary beam in the analyzer. However, the method needs careful consideration with respect to path integral fluctuations along the probing beam orbit to evaluate local magnetic fluctuation, similarly to density fluctuation measurements with a HIBP. Here, we present an analytic formula to estimate and calculate the path integral effects for different fluctuation patterns in the profile, the correlation length, the radial wavelength, and the poloidal mode number. As a result, it is found that a large distance between the plasma and the detector lessens the importance of the path integral effect, and that local fluctuation of the magnetic field can be properly detected with a HIBP. © *2005 American Institute of Physics.* [DOI: 10.1063/1.1889230]

I. INTRODUCTION

Heavy ion beam probes (HIBPs) have been applied to many kinds of plasma confinement devices, such as mirrors [Tandem Mirror Experiment (TMX)[1], GAMMA10[2]], a bumpy torus [Nagoya Bumpy Torus (NBT)[3]], a reversed field pinch [Madison Symmetric Torus (MST)[4]], tokamaks [Impurity Study Experiment (ISX-B)[5], Texas Experimental Tokamak (TEXT)[6], Japan Institute for Plasma Physics Tokamak (JIPP-TIIU)[7], T-10[8], JAERI's Fusion Torus (JFT-2M)[9]], and stellarators [Advanced Toroidal Facility (ATF)[10], Compact Helical System (CHS)[11], Large Helical Device (LHD)[12]]. This is because a HIBP has the unique capability of being able to simultaneously sense potential, density, and magnetic fields in the interiors of high temperature plasmas. As well, the highly temporal and spatial resolution with a HIBP allows for the detection of the fluctuations of these physical quantities. Until now, HIBPs have been mainly used to measure density and potential fluctuations[13] and the potential profile, and the results have contributed to the clarification of phenomena associated with plasma confinement, e.g., anomalous transport, barrier formation,[14] bifurcation and, transition.[15] However, few attempts have been made to use a HIBP to measure density profile,[16] magnetic field profile, and magnetic field fluctuations,[17,18] even though measurements of these physical quantities would be fascinating.

The measurement of a magnetic field is very attractive, because few diagnostics can measure the magnetic field in plasma. With HIBP measurements, the variation in the structure of a magnetic field is obtained from changes in beam orbits; however, it is difficult to ascertain the full orbit change. On the other hand, it is easy to measure the toroidal beam displacement at the detector, a displacement that is largely caused by magnetic fluctuation localized to the HIBP sample volume in an axisymmetric toroidal device. However, the problem is that some of the beam displacement reflects fluctuation along the beam orbit; a situation that is similar to that of density fluctuations. There are a number of reports regarding this contamination, called the "path integral effect"[19–21]; however, there are few reports regarding the path integral effects of magnetic field fluctuation measurements with a HIBP.

In this article, a model of the path integral effect is presented after a brief description of HIBP diagnostics. The model is used with several assumed profiles of magnetic fluctuations to predict the motion of the HIBP ions at the detector, and to determine the component of the signal due to local magnetic fluctuation at the sample location and the component due to the path effect. It is shown that the sensitivity to local fluctuations relative to the path effect can be improved by choosing a suitable position for the energy analyzer. The feasibility of the method is discussed, in terms of the minimum detectable fluctuation level with this method.

II. MATHEMATICAL PREPARATION AND CALCULATION MODEL

A. Principles of magnetic fluctuation measurements

A HIBP system consists of a beam injector or accelerator and an energy analyzer, as shown in Fig. 1(a). Usually, a single ionized heavy ion beam (or a primary beam) is injected into the plasma from a beam gun, and doubly ionized ions are created through electron impact ionization in the

[a]Author to whom correspondence should be addressed; electronic mail: akihiro@nifs.ac.jp

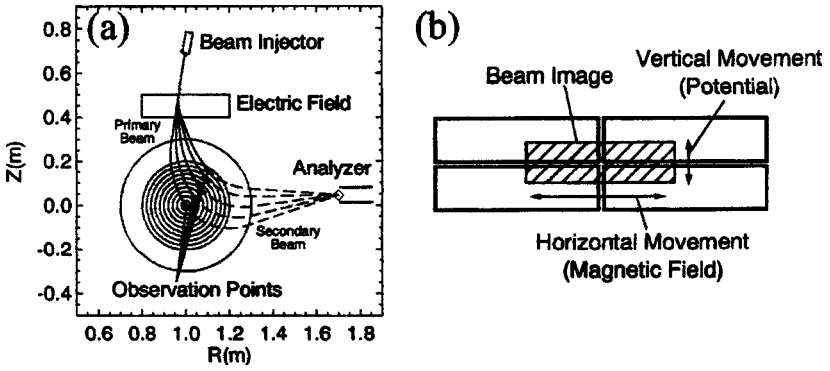

FIG. 1. (a) A schematic view of a HIBP system consisting of a beam injector, an energy analyzer, and beam sweep plates, and the assumed orbits in our calculations. The rectangular termed electric field means a region of a sweep plate to control the primary beam orbit and to change the observation point. (b) A schematic view of a split plate detector set in the energy analyzer to detect the secondary beam.

plasma. The doubly ionized beam (or secondary beam) comes out from the plasma and is detected at the energy analyzer. Usually a Proca and Green-type analyzer[22] is used as the energy analyzer, and the beam is detected with a so-called split plate detector [see Fig. 1(b)]. The detected beam intensity contains information on the plasma density at an observation point, while the vertical and horizontal movements on the detector plates give information on the potential and the magnetic field, respectively.

If the magnetic configuration is axisymmetric, as it is for an ideal tokamak, then the horizontal movement can be described in an analytic form, since the canonical momentum of the toroidal direction is conserved. The relation of momentum conservation along the primary orbit is written as

$$mR^2\dot{\phi} + qRA_\phi = qR_gA_{\phi g}. \tag{1}$$

Here, m is the beam ion mass, R the major radius, ϕ the toroidal angle, dot means the time derivative, q the charge of an electron, and A_ϕ the toroidal component of the vector potential. The right hand side shows an initial value, and $A_{\phi g}$, R_g are the toroidal component of the vector potential and the major radius at the beam gun (or beam injection point), respectively. For conciseness, the initial velocity in the toroidal direction is assumed to be zero, i.e., $\dot{\phi}_g = 0$. On the other hand, the law of conservation along the secondary orbit is expressed as follows:

$$mR^2\dot{\phi} + 2qRA_\phi = qR_sA_{\phi s} + qR_gA_{\phi g}, \tag{2}$$

where R_s and $A_{\phi s}$ represent the major radius and the vector potential at an observation point, respectively. After ionization, the beam ions experience an increase in the vector potential by $qR_sA_{\phi s}$. The toroidal displacement of the beam at the detector position can be obtained by integrating these two equations. Then, the toroidal angle displacement can be expressed in the following form:

$$\begin{aligned}\phi_D &= \int_0^{t_d}\dot{\phi}dt = \frac{1}{v}\int_0^{\ell_d}\dot{\phi}d\ell \\ &= \frac{qR_sA_{\phi s}}{mv}\int_{\ell_s}^{\ell_d}\frac{1}{R^2}d\ell + \frac{qR_gA_{\phi g}}{mv}\int_0^{\ell_d}\frac{1}{R^2}d\ell \\ &\quad - \frac{q}{mv}\int_0^{\ell_s}\frac{A_\phi}{R}d\ell - \frac{2q}{mv}\int_{\ell_s}^{\ell_d}\frac{A_\phi}{R}d\ell,\end{aligned} \tag{3}$$

where v is the magnitude of the velocity of a beam ion, which is assumed to be constant; namely, the effect of the plasma potential is neglected, and t_d is the time at which a beam ion reaches the detector position. The integral of time, t, is replaced by an integral about path length, ℓ, in this equation. The terms ℓ_s and ℓ_d are the path length on the beam orbit from the beam gun to the observation point and from the beam gun to the detector position, respectively. The fluctuated component of the toroidal angle of beam displacement can be written as

$$\begin{aligned}\tilde{\phi}_D &= \frac{qR_s\tilde{A}_{\phi s}}{mv}\int_{\ell_s}^{\ell_d}\frac{1}{R^2}d\ell + \frac{qR_g\tilde{A}_{\phi g}}{mv}\int_0^{\ell_d}\frac{1}{R^2}d\ell \\ &\quad - \frac{q}{mv}\int_0^{\ell_s}\frac{\tilde{A}_\phi}{R}d\ell - \frac{2q}{mv}\int_{\ell_s}^{\ell_d}\frac{\tilde{A}_\phi}{R}d\ell.\end{aligned} \tag{4}$$

Therefore, the fluctuation of the beam movement on the detector plate can be estimated using this formula by multiplying the major radius of the detector position R_d by the toroidal angle displacement $\tilde{\phi}_D$.

B. Calculation model

For normalization and to use nondimensional variables in the calculation, Eq. (4) is transformed into the following form:

$$\begin{aligned}\tilde{\phi}_D &= \frac{R_0}{r_L}\delta_0\hat{\phi}_D, \\ \hat{\phi}_D &\equiv \hat{R}_s\tilde{\alpha}_\phi(\hat{\mathbf{r}}_s)\int_{\hat{\ell}_s}^{\hat{\ell}_d}\frac{1}{\hat{R}^2}d\hat{\ell} + \hat{R}_g\tilde{\alpha}_\phi(\hat{\mathbf{r}}_g)\int_0^{\hat{\ell}_d}\frac{1}{\hat{R}^2}d\hat{\ell} \\ &\quad - \int_0^{\hat{\ell}_s}\frac{\tilde{\alpha}_\phi(\hat{\mathbf{r}})}{\hat{R}}d\hat{\ell} - 2\int_{\hat{\ell}_s}^{\hat{\ell}_d}\frac{\hat{\alpha}_\phi(\hat{\mathbf{r}})}{\hat{R}}d\hat{\ell}.\end{aligned} \tag{5}$$

Here, $r_L = mv/(qB_0)$, $\hat{R} = R/R_0$, $\hat{R}_s = R_s/R_0$, $\hat{R}_d = R_d/R_0$, $\hat{\ell} = \ell/R_0$. The parameters R_0 and B_0 are the major radius and toroidal magnetic field strength that characterize an experimental device, respectively. The function $\tilde{\alpha}_\phi$ is the normalized vector potential, of which the maximum is one, with δ_0 being the maximum level of $\tilde{A}_\phi/(B_0R_0)$. Hence, $\delta_0\tilde{\alpha}_\phi \equiv \tilde{A}_\phi/(B_0R_0)$. Note that $\tilde{\alpha}_\phi$ is a function of the position vector $\hat{\mathbf{r}}$; $\hat{\mathbf{r}}_s$ and $\hat{\mathbf{r}}_g$ are the position vectors at the observation point and at beam gun, respectively. $\hat{\phi}_D$ is the beam angle displacement to the toroidal direction normalized by $R_0\delta_0/r_L$. Then, the fluctuation power is written as

$$\langle \hat{\phi}_D^2 \rangle = A_1 + A_2 + A_3 + B_1 + B_2 + B_3 + B_4 + C_1 + C_2 + C_3. \tag{6}$$

Here the bracket $\langle \cdots \rangle$ means the ensemble average, and the symbols are

$$A_1 \equiv \langle (G_1 \hat{R}_s \tilde{\alpha}_\phi(\hat{\mathbf{r}}_s))^2 \rangle, \tag{7}$$

$$A_2 \equiv \langle (G_2 \hat{R}_g \tilde{\alpha}_\phi(\hat{\mathbf{r}}_g))^2 \rangle, \tag{8}$$

$$A_3 \equiv 2G_1 G_2 \hat{R}_s \hat{R}_g \langle \tilde{\alpha}_\phi(\hat{\mathbf{r}}_s) \tilde{\alpha}_\phi(\hat{\mathbf{r}}_g) \rangle, \tag{9}$$

$$B_1 \equiv -2G_1 \hat{R}_s \int_0^{\hat{\ell}_s} \langle \tilde{\alpha}_\phi(\hat{\mathbf{r}}_s) \tilde{\alpha}_\phi(\hat{\mathbf{r}}_1) \rangle \frac{1}{\hat{R}(\hat{\mathbf{r}}_1)} d\hat{\ell}_1, \tag{10}$$

$$B_2 \equiv -4G_1 \hat{R}_s \int_{\hat{\ell}_s}^{\hat{\ell}_d} \langle \tilde{\alpha}_\phi(\hat{\mathbf{r}}_s) \tilde{\alpha}_\phi(\hat{\mathbf{r}}_2) \rangle \frac{1}{\hat{R}(\hat{\mathbf{r}}_2)} d\hat{\ell}_2, \tag{11}$$

$$B_3 \equiv -2G_2 \hat{R}_g \int_0^{\hat{\ell}_s} \langle \tilde{\alpha}_\phi(\hat{\mathbf{r}}_g) \tilde{\alpha}_\phi(\hat{\mathbf{r}}_1) \rangle \frac{1}{\hat{R}(\hat{\mathbf{r}}_1)} d\hat{\ell}_1, \tag{12}$$

$$B_4 \equiv -4G_2 \hat{R}_g \int_{\hat{\ell}_s}^{\hat{\ell}_d} \langle \tilde{\alpha}_\phi(\hat{\mathbf{r}}_g) \tilde{\alpha}_\phi(\hat{\mathbf{r}}_2) \rangle \frac{1}{\hat{R}(\hat{\mathbf{r}}_2)} d\hat{\ell}_2, \tag{13}$$

$$C_1 \equiv \int_0^{\hat{\ell}_s} \int_0^{\hat{\ell}_s} \langle \tilde{\alpha}_\phi(\hat{\mathbf{r}}_1) \tilde{\alpha}_\phi(\hat{\mathbf{r}}_1') \rangle \frac{1}{\hat{R}(\hat{\mathbf{r}}_1)\hat{R}(\hat{\mathbf{r}}_1')} d\hat{\ell}_1 d\hat{\ell}_1', \tag{14}$$

$$C_2 \equiv 4 \int_{\hat{\ell}_s}^{\hat{\ell}_d} \int_{\hat{\ell}_s}^{\hat{\ell}_d} \langle \tilde{\alpha}_\phi(\hat{\mathbf{r}}_2) \tilde{\alpha}_\phi(\hat{\mathbf{r}}_2') \rangle \frac{1}{\hat{R}(\hat{\mathbf{r}}_2)\hat{R}(\hat{\mathbf{r}}_2')} d\hat{\ell}_2 d\hat{\ell}_2', \tag{15}$$

$$C_3 \equiv 4 \int_0^{\hat{\ell}_s} \int_{\hat{\ell}_s}^{\hat{\ell}_d} \langle \tilde{\alpha}_\phi(\hat{\mathbf{r}}_1) \tilde{\alpha}_\phi(\hat{\mathbf{r}}_2) \rangle \frac{1}{\hat{R}(\hat{\mathbf{r}}_1)\hat{R}(\hat{\mathbf{r}}_2)} d\hat{\ell}_1 d\hat{\ell}_2, \tag{16}$$

$$G_1 \equiv \int_{\hat{\ell}_s}^{\hat{\ell}_d} \frac{1}{\hat{R}(\hat{\mathbf{r}}_2)^2} d\hat{\ell}_2, \tag{17}$$

$$G_2 \equiv \int_0^{\hat{\ell}_d} \frac{1}{\hat{R}(\hat{\mathbf{r}})^2} d\hat{\ell}. \tag{18}$$

In these equations, $\hat{\mathbf{r}}_1, \hat{\mathbf{r}}_1', \hat{\mathbf{r}}_2, \hat{\mathbf{r}}_2', \hat{\mathbf{r}}$ are the functions of $\hat{\ell}_1, \hat{\ell}_1', \hat{\ell}_2, \hat{\ell}_2', \hat{\ell}$, respectively. A_1 represents the local fluctuation power of the magnetic field to be observed, while the other terms are considered contaminations; A_2 is the local fluctuation power at the beam gun, A_3 is the correlation between two local A terms, B_i the cross terms between the fluctuation in the orbits and at local points, and C_i the cross terms between primary and secondary orbits. G_1 and G_2 are geometrical factors which only depend on the beam orbit.

C. Model of cross correlation terms

In Eqs. (7)–(18), the path integral terms can be evaluated if the cross correlations with the vector potentials are given. The correlation term of $\langle \tilde{\alpha}_\phi(\hat{\mathbf{r}}_i) \tilde{\alpha}_\phi(\hat{\mathbf{r}}_j) \rangle$ is assumed as

$$\langle \tilde{\alpha}_\phi(\hat{\mathbf{r}}_i) \tilde{\alpha}_\phi(\hat{\mathbf{r}}_j) \rangle = P(\hat{\mathbf{r}}_i, \hat{\mathbf{r}}_j) \gamma(\hat{\mathbf{r}}_i, \hat{\mathbf{r}}_j) \Psi(\hat{\mathbf{r}}_i, \hat{\mathbf{r}}_j). \tag{19}$$

Here, P is the product of the amplitude of normalized fluctuations $\tilde{\alpha}_\phi(\hat{\mathbf{r}}_i)$, and $\tilde{\alpha}_\phi(\hat{\mathbf{r}}_j)$, γ and Ψ are the coherence and the cosine of the phase difference, respectively, between these fluctuations. A radial profile of amplitude of $\tilde{\alpha}_\phi(\hat{\mathbf{r}}_i)$, which is written as $\hat{P}_i$ in this article, is assumed to be, $\exp(-(\hat{r}-\hat{r}_0)^2/\hat{r}_w^2)$ in plasma; r is the minor radius, and r_0 is the radial position where the amplitude is a maximum; r_w is the width of the amplitude. The hat symbol of these variables means normalization by R_0. Outside the plasma, the radial profile of amplitude of $\tilde{\alpha}_\phi$ is assumed to be $\exp(-(\hat{a}-\hat{r}_0)^2/\hat{r}_w^2) \cdot (\hat{a}/\hat{r})^m$, as is seen in Ref. 17, where $\hat{a}$ is the minor radius of outermost magnetic surface normalized by R_0, m is the poloidal mode number.

The product of the fluctuation amplitude, P, is expressed as follows:

$$P = \hat{P}_i \cdot \hat{P}_j, \tag{20}$$

$$\hat{P}_i = \begin{cases} \exp(-(\hat{r}_i - \hat{r}_0)^2/\hat{r}_w^2) & r_i \leqslant \hat{a} \\ \exp(-(\hat{a} - \hat{r}_0)^2/\hat{r}_w^2) \cdot (\hat{a}/\hat{r}_i)^m & r_i > \hat{a} \end{cases}. \tag{21}$$

The coherence γ and the cosine of the difference in the phase Ψ between the fluctuations are assumed as

$$\gamma = \exp(-|\hat{\mathbf{r}}_i - \hat{\mathbf{r}}_j|^2/\hat{\ell}_c^2), \tag{22}$$

$$\Psi = \cos(m(\theta_i - \theta_j)) \cdot \cos((\hat{r}_i - \hat{r}_j)/(2\pi\hat{\lambda}_r)). \tag{23}$$

Here, $|\mathbf{r}_i - \mathbf{r}_j|$ is the distance between two points under consideration, ℓ_c the correlation length, m the poloidal mode number, θ_i, θ_j the poloidal angles, r_i, r_j the minor radii, λ_r the wavelength of fluctuation to the radial direction. The hat of these variables means normalization by R_0 as described above. We change the values of $\hat{r}_0$, $\hat{\ell}_c$, m, $\hat{\lambda}_r$ and investigate the effect of these parameters on the path integral terms in the function, $\hat{\phi}_D$.

III. CALCULATION RESULTS

A. Path integral effects for fluctuation patterns

Here we calculate path integral effects or contaminations for three fluctuation patterns to show the possibility of magnetic field measurements with a HIBP. The assumed HIBP geometry and orbits for the calculation are shown in Fig. 1(a); The beam injection point $(\hat{R}_g, \hat{Z}_g)$ is (1.0, 0.7), the detection point $(\hat{R}_d, \hat{Z}_d)$ is (1.7, 0.05) respectively. The cross section of the torus is circular, and the toroidal magnetic field is proportional to $1/\hat{R}$. The ratio of the major radius to the Larmor radius, R_0/ρ_L, is 2.3. Figure 2 upper shows assumed fluctuation patterns of vector potential $\tilde{\alpha}_\phi(\hat{\mathbf{r}})$ in the power function, $\hat{P}_i$. Here, we define $\hat{P}_i \equiv \exp(-(\hat{r}-\hat{r}_0)^2/\hat{r}_w^2)$, and consider three cases for $\hat{r}_0, \hat{r}_w$: (A) $\hat{r}_0 = 0.05$, $\hat{r}_w = 0.03$, the fluctuation profile has a peak near the center, (B) $\hat{r}_0 = 0.11$, $\hat{r}_w = 0.05$, a peak at the half radius, (C) $\hat{r}_0 = 0.17$, $\hat{r}_w = 0.05$, a peak near the edge. In order to give a perspective, the lower part of Fig. 2 shows the calculation results of the angle displacement, $\sqrt{\langle \hat{\phi}_D^2 \rangle}$, and the local term $\sqrt{A_1}$, which are shown as thick and thin lines, respectively. The assumed parameters

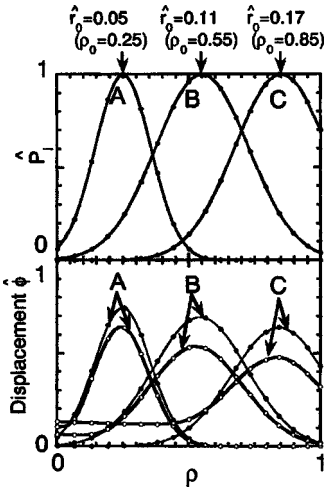

FIG. 2. Upper: Profiles of normalized fluctuation amplitude, $\hat{P}_i=\exp(-(\hat{r}-\hat{r}_0)^2/\hat{r}_w^2)$; $\hat{r}_0$ and ρ_0 mean the minor radius normalized by R_0 and the minor radius normalized by a, respectively, where the profile is a maximum. The profiles of three cases in which $\hat{r}_0, r_w$=(A) 0.05, 0.03, (B) 0.11, 0.05, (C) 0.17, 0.05, are shown. Lower: Profiles of normalized beam angle displacement to the toroidal direction, $\sqrt{\langle\hat{\phi}_D^2\rangle}$ (thick solid lines) and the square root of the local term A_1 in Eq. (7) (thin solid lines). The poloidal mode number $m=2$, correlation length $\hat{\ell}_c=0.1$, radial wave length $\hat{\lambda}_r=0.1$ are assumed in the calculation.

are $m=2$, $\hat{\ell}_c=0.1$, $\hat{\lambda}_r=0.1$ in this calculation. In case (A), no significant contamination can be found in either the central or the outer regime. This is because $\tilde{\alpha}_\phi \approx 0$ is valid except in the central regime and the path integral becomes small for the orbit to observe the outer regime of the plasma. However, in case (C) the path integral effect is large in the central regime. The beam orbit to observe the plasma center passes through the outer regime of the plasma where $\tilde{\alpha}_\phi$ has a significant value.

The sensitivity of the path integral effects is examined with respect to variations of the fluctuation parameters, correlation length, radial wavelength, and poloidal mode numbers. First, the effect of the correlation length $\hat{\ell}_c$ is investigated; $\hat{\ell}_c$ is changed from 0.01 to 0.2. The other parameters, $\hat{\lambda}_r$, m are fixed to 0.1, and 2, respectively. The calculated angle displacements for the profiles of fluctuation are shown in Fig. 3(a). The square root of the local term, $\sqrt{A_1}$, is also expressed as thin solid lines. In case (A), the difference between the beam angle displacement and the local term is small for any value of $\hat{\ell}_c$. In cases (B) and (C), if $\hat{\ell}_c \leqslant 0.01$, the beam angle displacement shows good agreement with the local term at the peak of the fluctuation. However, around the center of the plasma in case (C) the beam angle displacement does not show agreement with the local term.

Second, the results of a scan of $\hat{\lambda}_r$ are shown in Fig. 3(b), and are similar to a scan of $\hat{\ell}_c$. In this scan, m and $\hat{\ell}_c$ are fixed to 2 and 0.1, respectively. In case (A), the path integral effect is small; however, in case (C) it becomes larger. As the radial wavelength becomes smaller, the results show that the path integral effect becomes smaller. The path integral contribution around the center is more sensitive to $\hat{\lambda}_r$ than $\hat{\ell}_c$. If $\hat{\lambda}_r \leqslant 0.01$, the path integral terms become small in all cases from (A) to (C). For $\hat{\lambda}_r \leqslant 0.01$, the difference that remains near the plasma center in case (C) is due to the effect of the local term at the beam gun, A_2.

Finally, the results of a scan of m are shown in Fig. 3(c). The poloidal number m is changed from 1 to 3. In this case, $\hat{\ell}_c$, $\hat{\lambda}_r$ are fixed to 0.1, 0.1, respectively. In case (A), the difference of the beam angle displacement and the local term is small, and its dependence on m is also very small. However, in case (C), the difference at the plasma center for $m=1$ is very large. The angle between a primary and a secondary beam orbit is about $\pi/4$ radian in our case. When $m=1$, this angle corresponds to only one fourth of the wavelength; therefore, a reduction of the path integral cannot be expected. For $m=2$, the angle corresponds to one half of the wavelength, and so a reduction of path integral can be expected.

It is interesting to determine which terms are large in path integral terms. The profiles of these terms are shown in Fig. 4. In this case, the parameters for fluctuation, $\hat{\ell}_c$, $\hat{\lambda}_r$ and m are set to 0.1, 0.1 and 2, respectively. The largest term in path integral terms is B_2, which is the first order path integral term on the secondary beam path. Since the charge number of the secondary beam is twice of that of the primary beam, B_2 is 2 factors larger than B_1. The second largest term is B_1, which is of the same magnitude but the opposite sign of C_2

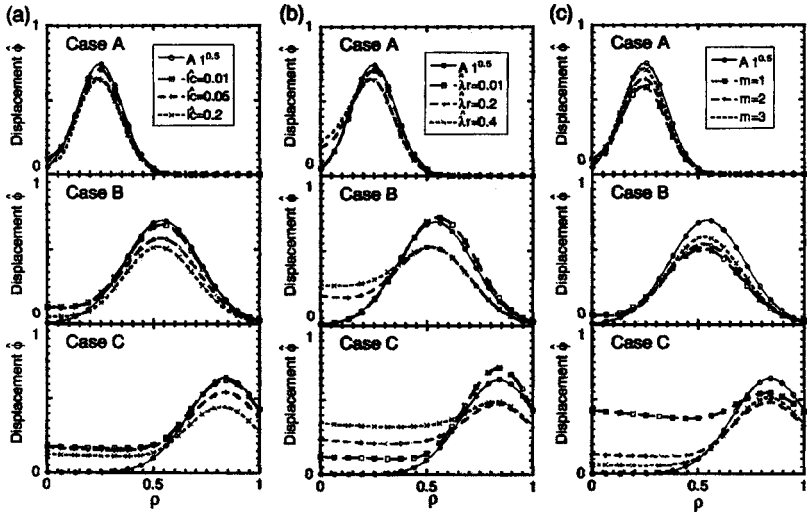

FIG. 3. (a) The calculation result of a scan of $\hat{\ell}_c$ with m and $\hat{\lambda}_r$ being fixed to 2 and 0.1, respectively. $\sqrt{A_1}$ is shown as solid lines. Dashed lines are the square of the normalized beam angle displacement, $\langle\hat{\phi}_D^2\rangle$. (b) The calculation result of a scan of $\hat{\lambda}_r$ with m and $\hat{\ell}_c$ being fixed to 2 and 0.1, respectively. (c) The calculation result of a scan of m with $\hat{\ell}_c$, $\hat{\lambda}_r$ being fixed to 0.1, and 0.1, respectively. The poloidal mode number m is changed from 1 to 3.

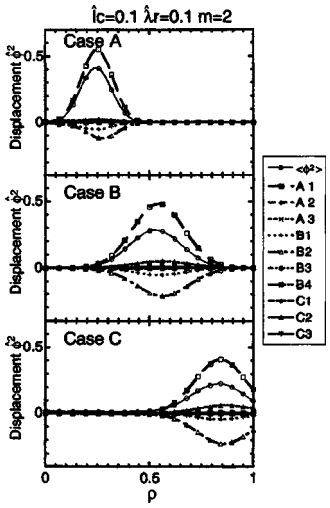

FIG. 4. An example of individual contributions of path integral components, from B_1 to C_3, in normalized angle displacement. The beam angle displacement $\langle\hat{\phi}_D^2\rangle$ is shown as a thin solid line. The largest contribution in path integral terms comes from B_2, which is the first order path integral term on the secondary beam path.

in this case; therefore B_1 is cancelled out with C_2. C_1, C_3 are small but cannot be ignored. Other terms are very small and can be ignored, except A_2 in case (C). Because the amplitude of the fluctuation is proportional to $1/\hat{r}^m$ outside of the plasma, the amplitude at the beam gun does not become sufficiently small in case (C). In the region near the plasma center, this term is the dominant one for beam angle displacement.

B. Effect of diagnostic position on magnetic fluctuation measurement

Equation (6) includes the geometrical factors G_1 and G_2. The squares of these factors appear in A_1 and A_2, and the factors are linear in B_1, B_2, B_3, and B_4. Hence, as G_1 becomes larger, the term A_1 increases more rapidly than B_1, B_2 and other terms. Thus, G_1 has the effect of magnifying the contribution of the local term A_1 to the fluctuation amplitude $\hat{\phi}_D^2$, and this leads to the relative reduction of path integral effects. The factor G_1 can be enhanced by setting the detector location farther away from the plasma, because the length of the path then becomes longer. Note $\tilde{\alpha}_\phi$ becomes negligibly small outside of the plasma; hence, the integral terms including $\tilde{\alpha}_\phi$ do not significantly contribute.

To investigate this geometrical (or HIBP configuration) effect, the path integral effect is calculated for several cases in which the major radii of the diagnostics points are different. The calculation results are shown in Figs. 5(a) and 5(b). The parameters of fluctuation are, $\ell_c=0.1$, $\lambda_r=0.1$, $m=2$. We consider two cases, (B) and (C), because in case (A) the path integral effect is already small. In Fig. 5(a), the profile of the beam angle displacement $\sqrt{\langle\hat{\phi}_D^2\rangle}$, and the local term $A_1^{0.5}$ are shown for the major radius of the diagnostic point $\hat{R}=1.53, 1.87, 2.38$. The magnitude of displacement is larger and the local term becomes dominant as the major radius of the detection point increases.

Figure 5(b) shows the dependence of individual path integral terms on the detector position. All terms are normalized by the square root of the local term, $A_1^{0.5}$, and their absolute values are shown in the figure. The path integral contribution $(A_1-\langle\hat{\phi}_D^2\rangle)^{0.5}/A_1^{0.5}$ is shown as a solid line. In case (B), the values of these terms at $\rho=0.55$ are shown, where the fluctuation amplitude is maximum, and in case (C) at $\rho=0.85$. For $\hat{R}\geqslant 1.7$, all terms decrease with the increase of $\hat{R}$, since G_1 becomes larger, while $B_2^{0.5}/A_1^{0.5}$ is increased when $\hat{R}$ is changed from 1.5 to 1.7.

The geometrical factor G_1 is the integral of $1/\hat{R}^2$; therefore, for a larger value of $\hat{R}$ an improvement of the path integral effect cannot be expected since the rate of G_1 rising becomes slower. In fact, this tendency is seen for the region of $\hat{R}\geqslant 2.3$ in Fig. 5(b). Consequently, $\hat{R}\approx 2.3$ is the best detector position for the accurate measurement of magnetic field fluctuation amplitudes.

IV. DISCUSSION

We have investigated here the feasibility of magnetic field fluctuation measurement using HIBPs by performing the calculation of beam movements for three assumed patterns of magnetic fluctuation. The findings are as follows: (1)

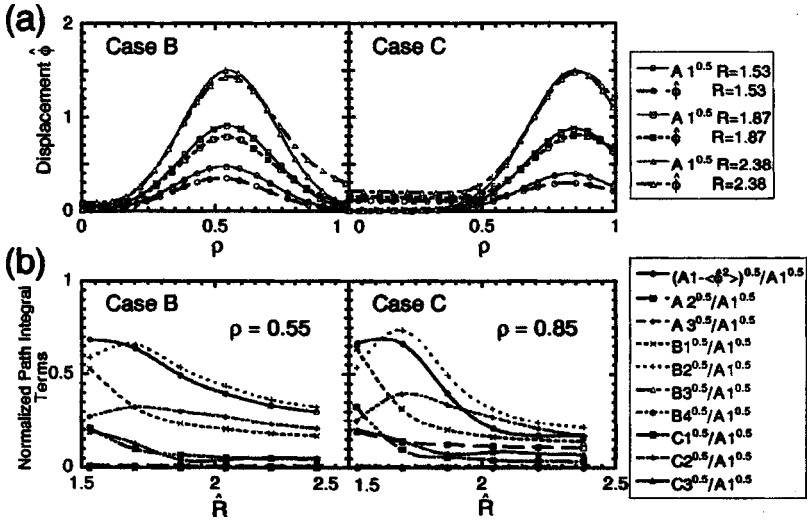

FIG. 5. A trial to find an appropriate position for the energy analyzer for magnetic field fluctuation measurements with a HIBP. (a) The dependence of beam angle displacement $\sqrt{\langle\hat{\phi}_D^2\rangle}$ on the position of the diagnostic point. Thin solid lines are profiles of the square root of the local term A_1. (b) The ratio of path integral terms to the local term, A_1, as a function of the major radius of the diagnostics point. The differences between the beam angle displacement and the local term, $(A_1-\langle\hat{\phi}^2\rangle)^{0.5}/A_1^{0.5}$, are shown as solid lines. The calculation is performed for cases B and C. The values presented are those at $\rho=0.55$ and at $\rho=0.85$ for cases B and C, respectively.

The path integral effect is so small that the fluctuation profile can be deduced, in cases where the magnetic field fluctuation is localized in the plasma core, independently of the fluctuation properties, e.g., $\hat{\ell}_c$, $\hat{\lambda}_r$, m. (2) However, if the fluctuation is localized in an outer region of the plasma, the path integral effect becomes larger; particularly, a false signal appears in the central regime of the plasma. (3) The path integral effects can be lessened if the detector position is kept as far as possible from the plasma.

The effect of magnetic field shielding due to a vacuum vessel is not considered in our calculations. If this shielding effect is taken into account, the path integral contribution associated with A_2, the fluctuation of the vector potential at the injection point, should be smaller. Actually in the case of edge-localized fluctuations, the signal distortion in the plasma core comes mainly from this effect. In Fig. 2, the false angle displacement in case (C) is reduced from 0.13 to 0.052 at the center if the term A_2 is neglected. Thus, the path integral effect is expected to be negligible for a magnetic field fluctuation localized in an outer region.

In HIBP measurements, a so-called split plate detector is used to measure the beam movement in the energy analyzer. A schematic view of the detector is shown in Fig. 1(b). In this detector, the horizontal beam displacement, d, can be expressed as $d=(\Delta w/2)(i_R-i_L)/(i_R+i_L)$, where i_R and i_L are the beam currents on the right and left plates, and Δw is the horizontal beam width. With this method, the beam movement of ~ 50 μm can be detected, with an assumption of $(i_R+i_L)=100$ nA, $\Delta w=5$ mm, and a minimum detectable current of 1 nA.

From the formula to describe the beam displacement $d_{\min}=\sqrt{\langle \hat{\phi}_D^2 \rangle}\times(R_0/r_L)\delta_{0,\min}R_d$, the minimum detectable fluctuation $\delta_{0,\min}(=\tilde{A}_\phi/(B_0R_0))$ is 2.6×10^{-5} for the case of $R_0=1$ m, $r_L\approx0.44$ m, $R_d=1.7$ m, $\sqrt{\langle \hat{\phi}_D^2 \rangle}\approx0.5$. This assumption corresponds to the case of a 70 keV cesium beam for a magnetic field strength $B_t=1$ T. Therefore, quite high sensitivity can be attained in magnetic field fluctuation measurements with HIBPs.

In conclusion, we have presented considerations of the path integral effects in magnetic field fluctuation measurements with a HIBP. We show that if the HIBP geometry is appropriately chosen, path integral effects can be negligible for a wide variety of fluctuation patterns; and it is better if the beam injection and detection points are located at a sufficient distance from the plasma. The results detailed are valid for axisymmetric magnetic configurations, and further consideration will be necessary for more realistic cases of nonaxisymmetrical configurations including toroidal ripples or stellarator magnetic configurations. This method, however, is quite promising since it provides a high sensitivity for magnetic fluctuations, less than 10^{-4}, with high resolutions of space ($\sim$ mm) and time ($\sim$ μs).

ACKNOWLEDGMENTS

The authors thank H. Iguchi, K. Matsuoka, S. Okamura and other members of the CHS-group for ongoing support.

[1] G. A. Hallock, R. L. Hickok, and R. S. Hornady, IEEE Trans. Plasma Sci. **22**, 341 (1994).
[2] K. Isii, IEEE Trans. Plasma Sci. **22**, 332 (1994).
[3] K. Takasugi, H. Iguchi, M. Fujiwara, and H. Ikegami, Jpn. J. Appl. Phys., Part 1 **23**, 364 (1984).
[4] U. Shah, K. A. Connor, J. Lei, P. M. Schoch, T. P. Crowley, J. G. Schatz, and Y. Dong, Rev. Sci. Instrum. **70**, 963 (1999).
[5] G. A. Hallock, A. J. Wootton, and R. L. Hickok, Phys. Rev. Lett. **59**, 1301 (1987).
[6] J. C. Forster, P. M. Schoch, R. L. Hickok, and W. C. Jennings, IEEE Trans. Plasma Sci. **22**, 359 (1994).
[7] Y. Hamada, A. Nishizawa, Y. Kawasumi, A. Fujisawa, and H. Iguchi, Fusion Eng. Des. **34,35**, 663 (1997).
[8] A. Melnikov, L. Eliseev, K. Razumova, I. Bondarenko, L. Krupnik, S. Khrebtov, A. Komarov, and A. Kozachek, J. Plasma Fusion Res. **3**, 46 (2000).
[9] T. Ido, Y. Hamada, A. Nishizawa, Y. Kawasumi, Y. Miura, and K. Kamiya, Rev. Sci. Instrum. **70**, 955 (1999).
[10] K. A. Connor, J. J. Zielinski, J. G. Schwelberger, and S. C. Aceto, Rev. Sci. Instrum. **63**, 4505 (1992).
[11] A. Fujisawa, H. Iguchi, S. Lee, T. P. Crowley, Y. Hamada, S. Kubo, H. Idei, H. Sanuki, and K. Itoh *et al.*, Phys. Plasmas **4**, 1357 (1997).
[12] A. Taniike, M. Sasao, A. Fujisawa, H. Iguchi, Y. Hamada, J. Fujita, M. Wada, and Y. Mori, IEEE Trans. Plasma Sci. **22**, 430 (1994).
[13] G. A. Hallock, P. M. Schoch, K. Saadatmand, R. L. Hickok, W. C. Jennings, and K. A. Connor, Rev. Sci. Instrum. **56**, 1038 (1985).
[14] T. Ido, K. Kamiya, Y. Miura, Y. Hamada, A. Nishizawa, and Y. Kawasumi, Phys. Rev. Lett. **88**, 055006 (2002).
[15] A. Fujisawa, H. Iguchi, T. Minami, Y. Yoshimura, H. Sanuki, K. Itoh, M. Isobe, S. Nishimura, C. Suzuki, K. Tanaka, M. Osakabe, I. Nomura, K. Ida, S. Okamura, and K. Toi *et al.*, Nucl. Fusion **41**, 575 (2001).
[16] A. Fujisawa, M. Kitazawa, A. Shimizu, S. Ohshima, and H. Iguchi, Rev. Sci. Instrum. **74**, 3335 (2003).
[17] V. J. Simicic, K. A. Connor, T. P. Crowley, R. L. Hickok, P. M. Schoch, A. J. Wootton, X. Z. Yang, and Y. Z. Zhang, Rev. Sci. Instrum. **61**, 3061 (1990).
[18] V. J. Simcic, T. P. Crowley, P. M. Schoch, A. Y. Aydemir, X. Z. Yang, K. A. Connor, R. L. Hickok, A. J. Wootton, and S. C. McCool, Phys. Fluids B **5**, 1576 (1993).
[19] D. W. Ross, M. L. Sloan, A. J. Wootton, P. M. Schoch, J. W. Heard, T. P. Crowley, R. L. Hickok, and V. Simcic, Rev. Sci. Instrum. **63**, 2232 (1992).
[20] J. W. Heard, T. P. Crowley, D. W. Ross, P. M. Schoch, R. L. Hickok, Jr., and B. Z. Zhang, Rev. Sci. Instrum. **64**, 1001 (1993).
[21] A. Fujisawa, H. Iguchi, S. Lee, and Y. Hamada, Rev. Sci. Instrum. **68**, 3393 (1997).
[22] G. A. Proca and T. S. Green, Rev. Sci. Instrum. **41**, 1778 (1970).